TRANSPORT PARAMETERS IN SUB-MICRON DEVICES

S. Bandyopadhyay, M. E. Klausmeier-Brown, C. M. Maziar, M. S. Lundstrom, and S. Datta.

School of Electrical Engineering
Purdue University
W. Lafayette, IN 47907

ABSTRACT

We present a new, *rigorous* technique for coupling Monte Carlo and drift-diffusion models for computationally efficient global device simulation. From regional Monte Carlo simulation, the position-dependent mobility, diffusion coefficient, and the energy-gradient field are evaluated for specific regions of several common device structures where hot electron effects are important. These are then used in a hybrid scheme for coupling Monte Carlo and drift-diffusion models so as to gain the advantages of each.

1. INTRODUCTION

A major drawback of global Monte Carlo simulation [1,2] is that the technique is difficult to apply to devices that contain low-field regions and is computationally demanding in many cases (e.g. when coupled with Poisson's equation or when carrier-carrier scattering is included). Because of this, drift-diffusion based device models continue to find wide application [3,4,5] - in spite of their well-known limitations [6]. Drift-diffusion models are simple and offer other benefits such as the capability to model recombination-generation currents and are also more suitable for studying capacitive effects. The major shortcoming of the drift-diffusion formalism is that it cannot model hot carrier effects, especially non-local effects such as velocity overshoot. Fortunately, such effects are absent in the low-field regions of a device, where Monte Carlo is inefficient. Consequently, these regions can be accurately modeled by conventional drift-diffusion formalism. It is only the high-field regions that require Monte Carlo, and this presents no serious problem since Monte Carlo is computationally efficient in these regions. Recently a new technique has been proposed [7,8] that couples Monte Carlo and drift-diffusion models in order to obtain the advantages of each. In this technique (hybrid technique), only the high-field regions of a device are simulated by Monte Carlo

and the low field regions are described by a field-independent mobility. From the simulation data for the high-field regions, a position-dependent mobility and diffusion coefficient are extracted and used in the conventional drift-diffusion equation to model the entire device. However, the method for extracting mobility and diffusion coefficient in the existing technique is ad hoc and it is difficult to judge its validity. In this paper, we present a new, *rigorous* technique for extracting such transport parameters from regional Monte Carlo simulations. We relate the transport parameters to the carrier distribution function, and evaluate such parameters within representative sub-micron structures.

The objective of this work is to present a rigorous prescription for evaluating transport parameters in short devices where hot carrier effects are important. The motivation for the objective arises from the observation that the hybrid technique is computationally efficient and has the potentiality to evolve as a viable scheme for accurate modeling of hot carrier effects. Yet, the existing techniques [7,8] are non-rigorous and therefore cannot exploit the full potentiality of the hybrid scheme. The technique that we present is rigorous, and at the same time, requires no more computational effort than the existing technique. Our technique is rigorously derived from the Boltzmann Transport Equation (BTE). As a result, transport variables such as current density, carrier density and carrier temperature evaluated by our technique are expected to be of general validity and their accuracy determined solely by the sophistication of the Monte Carlo program.

We begin in Sec. 2 by describing the theory of regional Monte Carlo simulation. We also demonstrate that the drift-diffusion equations are exact *if* the correct mobility and diffusion coefficient are used (an additional parameter termed the energy-gradient field is also required). We then show how these parameters can be evaluated using the results of Monte Carlo simulations. In Sec. 3 we illustrate the technique by computing drift-diffusion parameters for various device structures. These examples illustrate how the distribution function and the transport coefficients (mobility, diffusion coefficient and energy-gradient field) vary with position in typical device structures. Finally, the contributions and main findings of the paper are summarized in Sec. 4.

2. THEORY

In regional Monte Carlo analysis [7], portions of the device for which drift-diffusion is thought to be inapplicable are first identified. Monte Carlo simulation is then performed for such regions by assuming a distribution function $f_1(\vec{k})$ at the left boundary and a distribution function $f_2(\vec{k})$ at the right boundary. This procedure yields the electron density $n(\vec{x})$ and the ensemble velocity $v(\vec{x})$ from which a position-dependent mobility $\mu(\vec{x})$ and a diffusion coefficient $D(\vec{x})$ are extracted.

The current, carrier density, and average carrier velocity computed by Monte Carlo simulation are related by

$$J_i = -qn(\vec{x})\, v_i(\vec{x}) . \tag{1}$$

In principle, it is possible to solve this equation directly to obtain J_i and $n(\vec{x})$, using the $v_i(\vec{x})$ computed by Monte Carlo. However, when the equation is solved iteratively with Poisson's equation, the electric field inside the device may change with each successive iteration, and the Monte Carlo simulation has to be re-run each time to compute the new $v_i(\vec{x})$. In that case, it is advantageous to recast equation (1) in the form of a drift-diffusion equation, involving parameters such as mobility and diffusion coefficient. These parameters do not change very much with the electric field unless the distribution function changes drastically. (For instance, in the moderate field limit, $v_i(\vec{x})$ is approximately proportional to the electric field, but mobility is relatively independent of the electric field). Such parameters are thus expected to be far less sensitive to changing electric fields than $v_i(\vec{x})$, so that the Monte Carlo simulation need not be run everytime and convergence could be achieved faster. The problem then is to recast equation (1) *correctly* in the form of a drift-diffusion equation involving transport parameters.

We wish to choose μ and D in a conventional drift-diffusion equation,

$$J_i = q\mu(\vec{x})n(\vec{x})\mathcal{E}_i(\vec{x}) + qD_i(\vec{x})\frac{\partial n(\vec{x})}{\partial \vec{x}_i} , \tag{2}$$

where $\mathcal{E}_i$ is the electric field, so that the $n(\vec{x})$ and $\vec{v}(\vec{x})$ obtained by Monte Carlo analysis are recovered. It is apparent that for a given $n(\vec{x})$ and $v(\vec{x})$ there are numerous ways to choose $\mu(\vec{x})$ and $D(\vec{x})$ so that (1) and (2) are equal. One method would be to assume the Einstein relation,

$$D(\vec{x}) = (kT/q)\mu(\vec{x}) \tag{3}$$

where T is the lattice temperature. Using (1) - (3) we find

$$v(\vec{x}) = -\mu(\vec{x})\left[\mathcal{E}(\vec{x}) + \frac{kT}{q}\frac{\partial}{\partial \vec{x}} \ln n(\vec{x})\right] \tag{4}$$

which gives $\mu(\vec{x})$ and $D(\vec{x})$ as a unique function of $\mathcal{E}(\vec{x})$, $n(\vec{x})$ and $v(\vec{x})$.

This prescription for finding μ and D from n and $\vec{v}$ is straightforward and simple but is not rigorous. The use of the Einstein relation is questionable; even for homogeneous electric fields one should replace the lattice temperature T by the electron temperature T_e when the field is large. Consequently, only the total current is correctly evaluated - the diffusion current component is not. Moreover, μ and D obtained in this way are not the true physical parameters, they are simply chosen so that (2) reproduces the carrier density and velocity obtained by Monte Carlo analysis. As a result it is difficult to obtain

insight into the expected variations of these parameters within an arbitrary device.

We now reformulate the conventional drift-diffusion equations and describe a method for obtaining the drift-diffusion transport parameters. *This technique can be justified rigorously from the Boltzmann Equation and is of general validity.* Steady-state electron transport is described by a Boltzmann Transport Equation of the form:

$$\frac{1}{\hbar}\frac{\partial E}{\partial k_j}\frac{\partial f}{\partial x_j} - \frac{q\mathcal{E}_j}{\hbar}\frac{\partial f}{\partial k_j} = \left[\frac{\partial f}{\partial t}\right]_{coll}, \tag{5}$$

(q is the magnitude of the electronic charge, a positive quantity). As shown in the appendix, the first moment of this equation can be expressed in the form

$$J_i = qn\mu_{ij}(\mathcal{E}_j + \mathcal{E}'_j) + qD_{ij}\frac{\partial n}{\partial x_j}, \tag{6}$$

where summation over repeated indices is implied. Comparing (6) with the conventional drift-diffusion equation, we observe that an additional parameter, termed the energy-gradient field $\mathcal{E}'$, is required in order to correctly describe carrier transport in drift-diffusion form. The importance of this term has been discussed extensively in the literature [9]. This term is required to model the non-local effects of spatial transients which influence such phenomena as velocity-overshoot. Equation (6) is exact *if* the transport parameters, μ, D, and $\mathcal{E}'$, are evaluated from the distribution function as described below.

To evaluate the transport parameters in (6) the carrier distribution function $f(\vec{x},\vec{k})$ must be known in the regions of interest. Monte Carlo simulation provides a means for determining $f(\vec{x},\vec{k})$ in these regions. From the results of Monte Carlo simulation, we evaluate the zeroth moment of the distribution function (related to the average carrier density)

$$n(\vec{x}) = \frac{1}{\Omega}\sum_{\vec{k}} f(\vec{x},\vec{k}), \tag{7}$$

the first moment (the average carrier velocity),

$$\langle v_i(\vec{x})\rangle = \sum_{\vec{k}} f(\vec{x},\vec{k})\left[\frac{1}{\hbar}\frac{\partial E}{\partial k_i}\right] \Big/ \sum_{\vec{k}} f(\vec{x},\vec{k}), \tag{8}$$

and the second moment (the component of the average kinetic energy per carrier along the field),

$$\langle u_{ij}(\vec{x})\rangle = \frac{1}{2}\sum_{\vec{k}} f(\vec{x},\vec{k})\frac{\partial E}{\partial k_i}k_j \Big/ \sum_{\vec{k}} f(\vec{x},\vec{k}), \tag{9}$$

where Ω is the sample volume and $\vec{\nabla}_k E/\hbar$ gives the velocity of an electron with wave vector $\vec{k}$. As shown in the appendix, the transport parameters in the drift-diffusion equation, (6), are obtained by

the following prescription:

$$\mu_{ij}(\bar{x}) = \frac{-\langle v_i(\bar{x})\rangle}{\mathcal{E}_j + \frac{2}{qn(\bar{x})}\frac{\partial}{\partial x_i}(u_{ij}n)}, \tag{10}$$

$$D_{ij} = \frac{2}{q}\mu_{ik}u_{kj}, \tag{11}$$

and

$$\mathcal{E}'_j = \frac{2}{q}\frac{\partial}{\partial x_i}u_{ij}. \tag{12}$$

Equation (6) can now be used for device simulation with μ, D and $\mathcal{E}'$ obtained from (10) - (12) using (7) - (9) which are evaluated from the distribution function (computed, for example, by regional Monte Carlo simulation). This procedure for evaluating the transport parameters is valid for low and high-field transport under spatially homogeneous or nonhomogeneous conditions. The procedure is valid even when nonparabolicity of the band, and multiple valley occupancy must be considered. Such effects are already taken into account when evaluating v_i and u_{ij} from (8) and (9). Note that under low-field conditions, $u_{ij} = \frac{1}{2}kT\delta_{ij}$ (electron temperature is both isotropic and independent of position) so that $\mathcal{E}' = 0$ and (11) reverts to the conventional Einstein relation (Eq. 3). Under these conditions, the usual drift-diffusion equations are recovered. Under high-field spatially uniform conditions, $\mathcal{E}' = 0$ so that (6) reverts to a conventional drift-diffusion equation (Eq. 2) with field-dependent μ and D. Under spatially nonuniform conditions, such as those that frequently occur in devices, the energy-gradient field can be quite important and must be considered during spatial transients. It may either aid or oppose the applied electric field.

3. EXAMPLES

In this section, we apply the rigorous technique presented in the previous section in order to evaluate $\mu(\bar{x})$, $D(\bar{x})$, and $\mathcal{E}'(\bar{x})$ within typical GaAs and AlGaAs/GaAs device structures. The distribution function was first evaluated by an ensemble Monte Carlo technique similar to that described by Williams [10] then (7) - (12) were applied to evaluate the transport parameters. The examples were chosen to illustrate transport effects in two recently proposed structures both of which were considered for potential application as high-speed devices. A one-dimensional structure is assumed, with the electric field in the $-\hat{x}$ direction and μ_{xx}, D_{xx}, and $\mathcal{E}_{xx}$ are evaluated.

The first example to be discussed illustrates transport effects in the base of a Ballistic Base Heterojunction Bipolar Transistor (BBHBT) [11] where electrons are injected into the base from a "ballistic launching ramp". The ramp imparts high initial velocities to

the electrons and thereby reduces base transit time. The structure consists of a 0.25 μm section of GaAs with an electric field of 10^4 v/cm and an absorbing contact at the right which represents the reverse-biased collector junction. Carriers are injected from a velocity-weighted Maxwellian at the right with a minimum kinetic energy of 4kT to simulate carrier injection across a 4kT ballistic launching ramp. The results of Monte Carlo simulation and transport parameter extraction are displayed in Figs. 1a - 1l. Since carriers are injected with high energy (well above the threshold for polar optical phonon emission but not high enough for intervalley transfer to dominate) the main scattering event is again polar optical phonon emission. This type of scattering does not spread the distribution function since it favors small-angle scattering which allows the carriers to stream. In fact, at an energy of 4kT, the probability that $\cos\theta \sim 1$ (θ is the scattering angle) is about 70 times larger than the probability that $\cos\theta \sim 0$ [15]. As a result, the distribution function closely approximates a δ function at a velocity corresponding to the injection energy.

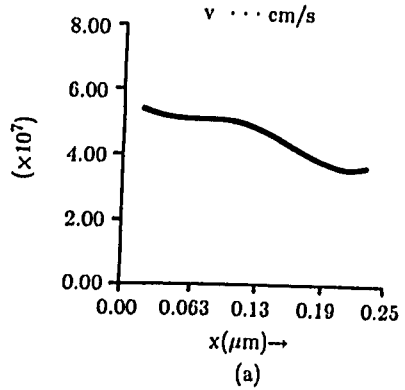

1a. Average velocity versus position for example 1. The structure is a 0.25 μm section of GaAs with a 10^4v/cm electric field and a ballistic launching ramp of 4kT at the left.

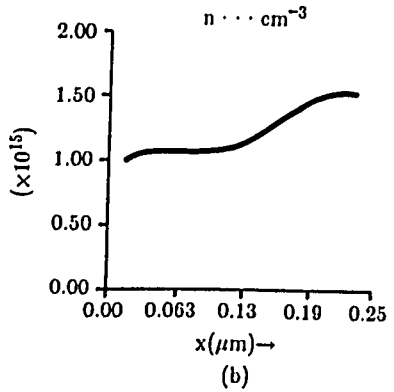

1b. Average carrier density versus position for example 1.

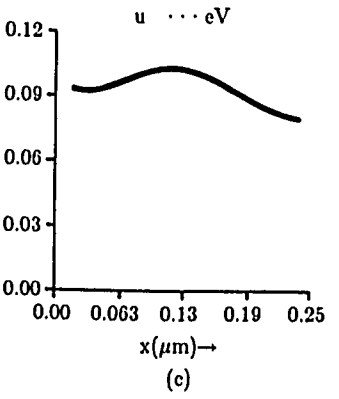

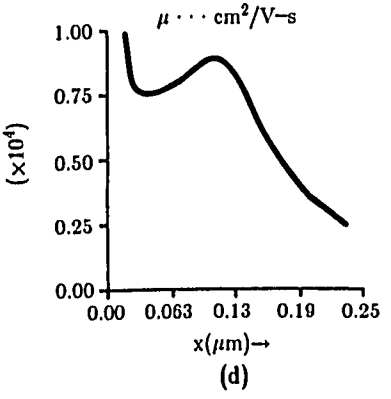

1c. Longitudinal component of average kinetic energy per carrier versus position for example 1.

1d. Mobility versus position for example 1.

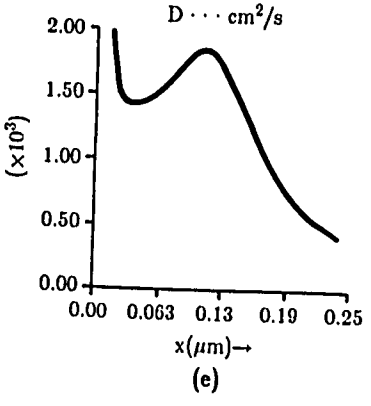

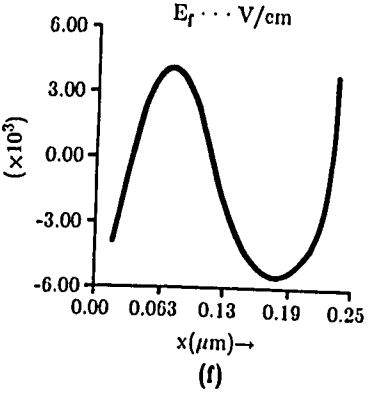

1e. Diffusion coefficient versus position for example 1.

1f. Energy-gradient field versus position for example 1.

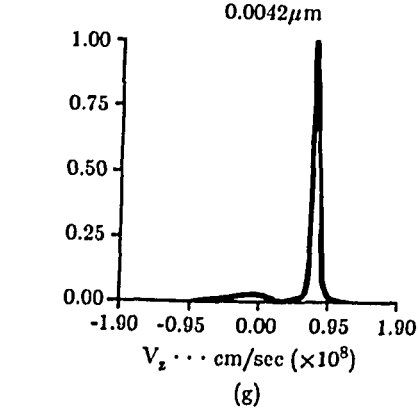

(g)

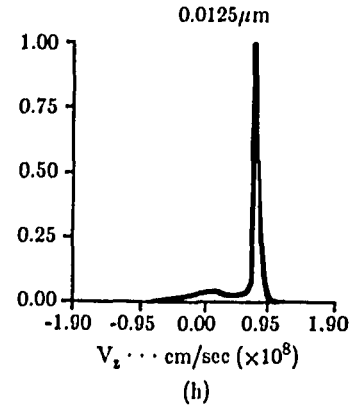

(h)

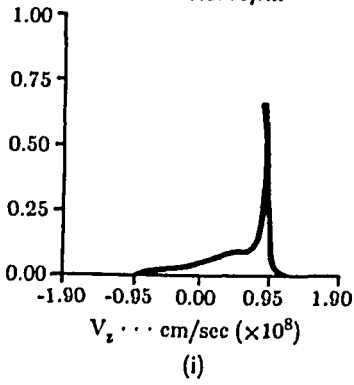

(i)

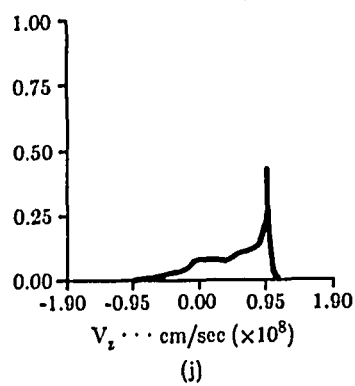

(j)

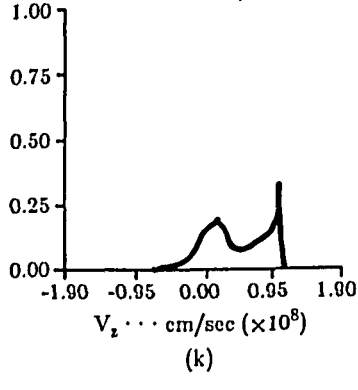

(k)

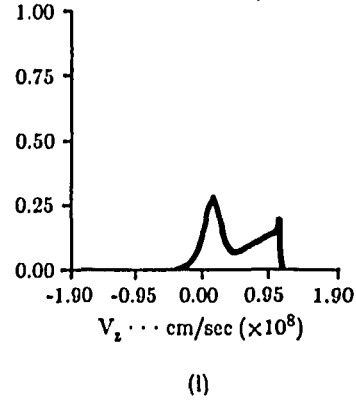

(l)

1g-l. Distribution function versus position for example 1.

As the average energy drops due to polar optical phonon emission, the anisotropy in the scattering mechanism is also reduced [12] and the distribution function spreads. Finally when intervalley scattering sets in, the distribution function spreads rapidly because of the randomizing nature of this scattering. Associated with the onset of intervalley scattering is the rapid degradation of mobility as seen in Fig. 1d. The x-directed kinetic energy component u_{xx} is relatively constant until intervalley transfer occurs; as a result D_{xx} tracks μ_{xx} but falls more rapidly with the onset of intervalley transfer. The energy-gradient field undergoes complicated variation since carriers enter with substantial kinetic energy, lose some due to collisions, are then accelerated in the field, and finally lose kinetic energy when intervalley transfer occurs. The energy-gradient field aids, then opposes, then aids, and finally opposes the real field; for most of the structure its magnitude is a substantial fraction of the real field.

The next example chosen is a repeated velocity overshoot structure (staircase structure) [13]. The Monte Carlo simulation was performed with periodic boundary conditions. Each section was taken to be 6000 Å long and the step-height was adjusted to 0.1 ev in order to inject carriers within the collision-free-window [14]. The applied electric field was 4.2 kv/cm. The transport variables and the results of the transport parameter extraction are displayed in Figs. 2b-2g. As shown in Fig. 2d, u_{xx} rapidly falls at the beginning due to frequent emission of polar optical phonons until a quasi-steady-state situation is reached. The mobility shown in Fig. 2e undergoes complicated variations; its rapid rise at the right end of the section is an artifact of the "anticipatory effect" [15]. Because of the steep drop in the potential at the right end of the stair-step, the electron ensemble in this region is composed almost entirely of particles traveling in the forward direction. This raises the average velocity and causes the rise in mobility. The average mobilty in the structure is however only about 6800 $cm^2/v-sec$ which is about 15 % less than the mobility in intrinsic GaAs at the applied field of 4.2 kv/cm.

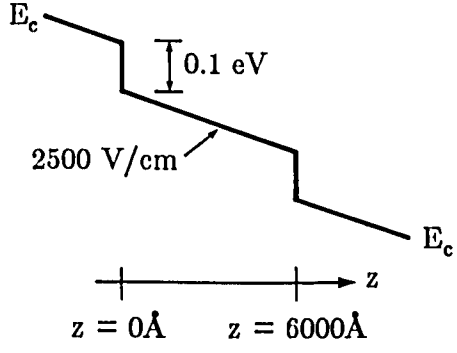

2a. Energy band diagram for a staircase heterostructure.

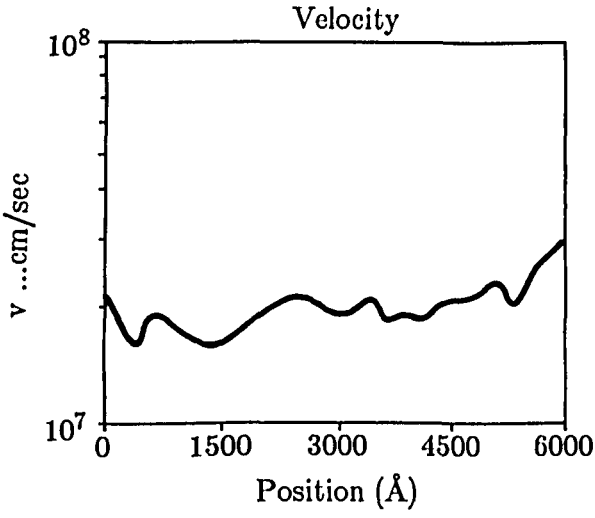

2b. Average velocity versus position for example 2.

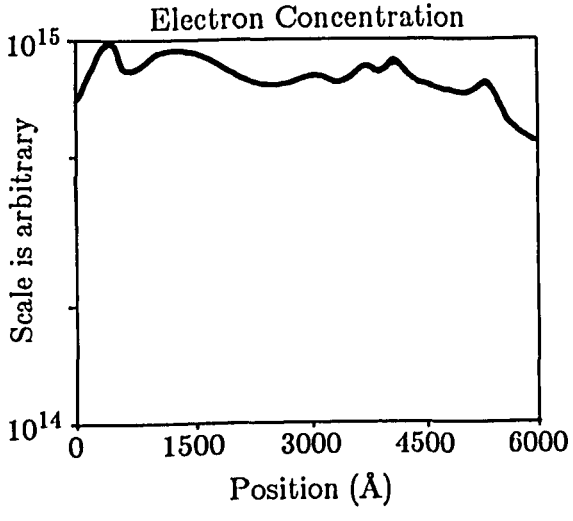

2c. Average carrier density versus position for example 2.

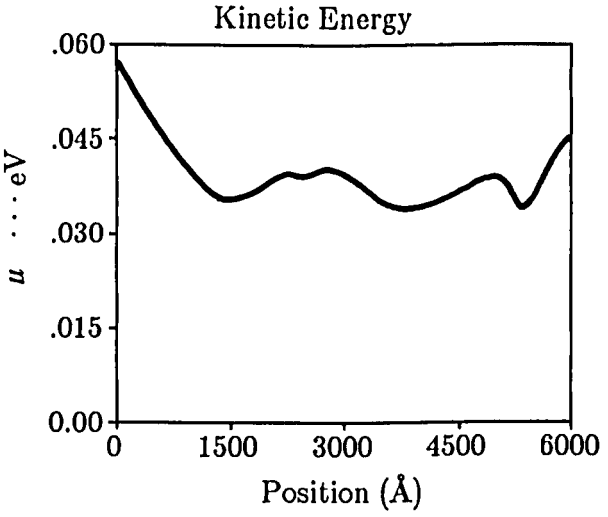

2d. Longitudinal component of average kinetic energy per carrier versus position for example 2.

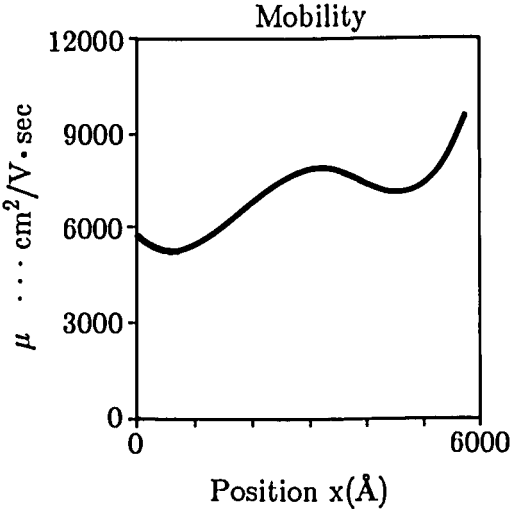

2e. Mobility versus position for example 2.

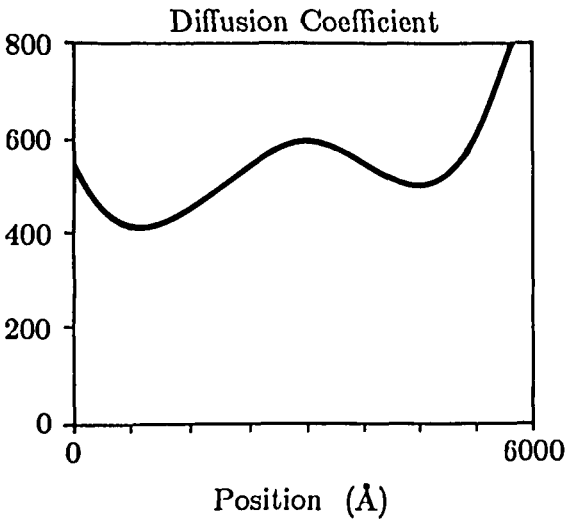

2f. Diffusion coefficient versus position for example 2.

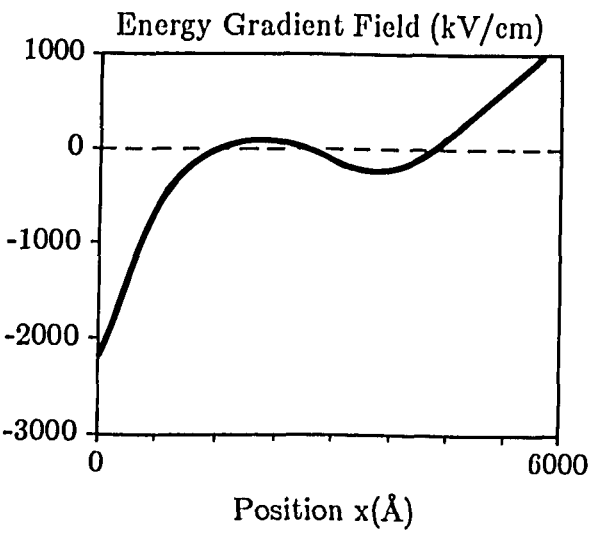

2g. Energy-gradient field versus position for example 2.

The diffusion coefficient shown in Fig. 2f is extremely high throughout the structure and consequently the diffusion current is a significant fraction of the total current, especially at the left end where the gradient in the carrier concentration is also high.

The energy-gradient field is very large and roughly equal to the applied field at the left end. Also its direction is such that it aids the applied field. Consequently, the velocity shown in Fig. 2b is somewhat higher at the left end.

4. SUMMARY

In this paper we have presented a rigorous prescription for evaluating transport coefficients in ultrasmall structures. These can be used in a computationally efficient and rigorous technique for simulating hot carrier transport in typical sub-micron devices. Several example computations were performed in order to illustrate the technique for device structures that are of interest. The results provide insight into the nature of carrier transport within such devices and provide quantitative estimates for drift-diffusion transport parameters in such structures.

Acknowledgement

This work was supported by the Semiconductor Research Corporation under Contract No. 83-01-001.

REFERENCES

[1] GLISSON, T.H., WILLIAMS, C.K., HAUSER, J.R., LITTLEJOHN, M.A.,
VLSI Microstructure Science, Vol. 5, Ch. 3, pp. 95-145, 1982.

[2] PRICE, P.J.,
Semiconductors and Semimetals Vol. 14, p. 249, Academic Press, New York, 1979.

[3] LUNDSTROM, M.S., and SCHUELKE, R.J.,
IEEE Trans. Electron Dev., Vol. ED-30, pp. 1151-1159, 1983.

[4] KURATA, M., and YOSHIDA, J.,
IEEE Trans. Electron Dev., Vol. ED-31, pp. 467-473, 1984.

[5] YOKOYAMA, K., TOMIZAWA, M., and YOSHII, A.,
IEEE Trans. Electron Dev., Vol. ED-31, pp. 1222-1229, 1984.

[6] See, for example, HESS, K.,
Advances in Electronics and Electron Physics, Vol. 59, pp. 239-290, Academic Press, New York, 1984.

[7] PARK, Y.J., NAVON, D.H., and TANG, T.W., IEEE Trans. Electron Dev., Vol. ED-31, p. 1274, 1984.

[8] NGUYEN, P.T., NAVON, D.H., and TANG, T.W., IEEE Trans. Electron Dev., Vol. ED-31, p. 783, 1985.

[9] See, for example, LANDSBERG, P.T., J. Appl. Phys., Vol. 56 (4), pp. 1119-1122, 1984.

[10] WILLIAMS, C.K., Ph. D. Thesis, N. Carolina State Univ., 1982.

[11] ANKRI, D., and EASTMAN, L.F., Electron Lett., Vol. 18, p. 750, 1982.

[12] LEBURTON, J.P., and HESS, K., Phys. Rev. B., Vol. 26, p. 5623, 1982.

[13] COOPER, J.A., CAPASSO, F., and THORNBER, K.K., IEEE Elec. Dev. Lett.,, Vol. EDL-3, pp. 407-408, 1982.

[14] BRENNAN, K., and HESS, K., IEEE Elec. Dev. Lett.,, Vol. EDL-4, pp. 419-421, 1983.

[15] GOLIO, J.M., TREW, R.J., TISCHLER, M., LITTLEJOHN, M.A., and HAUSER, J.R., abstract, Device Research Conf., 1983.

APPENDIX

In this appendix, we derive the transport equation (6) from the Boltzmann Transport Equation (BTE); the validity of the BTE is assumed, but no further assumptions are made. The BTE is written as

$$\frac{1}{\hbar}\frac{\partial E}{\partial k_j}\frac{\partial f}{\partial x_j}-\frac{q\mathcal{E}_j}{\hbar}\frac{\partial f}{\partial k_j}=\sum_{\vec{k}'}S(\vec{k}',\vec{k})f(\vec{k}')[1-f(\vec{k})]-S(\vec{k},\vec{k}')f(\vec{k})[1-f(\vec{k}')], \quad (A1)$$

where $f(\vec{x}, \vec{k})$ is the electron distribution function, $S(\vec{k},\vec{k}')$ is the rate of scattering from the state $\vec{k}$ to the state $\vec{k}'$ and $\frac{1}{\hbar}\frac{\partial E}{\partial k_j}$ is the velocity v_j. Summation over the repeated index j is implied. We now take the first moment by multiplying (A1) by k_i and summing over $\vec{k}$ to obtain,

$$\sum_{\vec{k}}\frac{1}{\hbar}\frac{\partial E}{\partial k_j}k_i\frac{\partial f}{\partial x_j}-\sum_{\vec{k}}\frac{q\mathcal{E}_j}{\hbar}k_i\frac{\partial f}{\partial k_j}$$

$$=\sum_{\vec{k}}\sum_{\vec{k}'}k_i\left\{S(\vec{k}',\vec{k})f(\vec{k}')[1-f(\vec{k})]-S(\vec{k},\vec{k}')f(\vec{k})[1-f(\vec{k}')]\right\} \quad (A2)$$

Equation (A2) can be expressed as

$$\frac{\partial}{\partial x_j}(2n\, u_{ij}) + q\mathcal{E}_i n = -\left(\frac{dp_i}{dt}\right)_{coll} \tag{A3a}$$

where

$$2nu_{ij} = \frac{1}{\Omega}\sum_{\vec{k}} f(\vec{x},\vec{k})\frac{\partial E}{\partial k_j}k_i \tag{A3b}$$

Ω is the volume element, and

$$\left(\frac{dp_i}{dt}\right)_{coll} = \frac{1}{\Omega}\sum_{\vec{k}}\sum_{\vec{k}'}(\hbar k_i - \hbar k_i')S(\vec{k},\vec{k}')f(\vec{k})[1-f(\vec{k}')] \tag{A3c}$$

is the rate of loss of electron momentum due to collisions.

We now take as the defining relation for the mobility:

$$J_i = -\mu_{ij}\left(\frac{dp_j}{dt}\right)_{coll}. \tag{A4}$$

When (A4) is solved for $\left(\frac{dp_i}{dt}\right)_{coll}$, the result can be used in (A3a) to obtain

$$J_i = qn\mu(\mathcal{E}_i + \mathcal{E}_i') + qD_{ij}\frac{\partial n}{\partial x_j} \tag{A5}$$

which is the desired result. The diffusion coefficient in (A5) is

$$D_{ij} \equiv \mu_{ik}(2u_{kj}/q) \tag{A6}$$

and the energy-gradient field,

$$\mathcal{E}_j' \equiv \frac{2}{q}\frac{\partial}{\partial x_i}u_{ij}. \tag{A7}$$

An alternative expression for μ_{ij} that is more convenient to compute by Monte Carlo simulation can be obtained by writing

$$J_i = -qn\langle v_i\rangle \tag{A8}$$

which may be inserted in (A4) to solve for the momentum loss term. When this result is inserted in (A3a), the mobility is obtained as

$$\mu_{ij}(\vec{x}) = -\langle v_i(\vec{x})\rangle/(\mathcal{E}_j(\vec{x}) + \frac{2}{qn(\vec{x})}\frac{\partial}{\partial x_i}(u_{ij}n)). \tag{A9}$$